

SIMULATION TECHNIQUES FOR ARRIVAL PROCEDURE DESIGN IN CONTINUOUS DESCENT OPERATION

Daichi Toratani
Navinda Kithmal Wickramasinghe
Hiroko Hirabayashi

Air Traffic Management Department
Electronic Navigation Research Institute (ENRI)
7-42-23 Jindaijihigashimachi
Chofu, Tokyo 182-0012, JAPAN

ABSTRACT

Continuous descent operation (CDO) is fuel-saving noise-abating arrival procedures that are used at the Kansai International Airport (KIX). However, CDO can only be performed at night so as not to disturb airflow during heavy daytime traffic. Altitude window has been proposed as a solution to expand the CDO operations. The operational conditions surrounding the arrival route, such as the percentages of aircraft types and the wind conditions, should be adequately considered while designing the altitude window. This study describes the simulation techniques that are used to formulate this design. A fast-time simulation (FTS) is exhibited to calculate the maximum possible range of the vertical-CDO trajectory. A performance-review method for the altitude window is also depicted using an FTS. Exemplary simulations are conducted using the actual KIX data. Finally, the application of a review method for the altitude window is discussed to develop the total design process.

1 INTRODUCTION

Continuous descent operations (CDO) are a key method to improve the arrival procedures for commercial aircraft (International Civil Aviation Organization 2010). Conventionally, an arriving aircraft descends step-by-step according to the instructions of an air traffic controller; in a CDO, however, the aircraft descends continuously while maintaining an idle thrust. By eliminating the leveling-off segment at a low altitude, CDO can reduce the fuel consumption and noise pollution. In Japan, CDO procedures have been implemented at the following three airports: Kansai International Airport (KIX), Kagoshima Airport (KOJ), and Naha Airport (OKA). This study focuses on the CDO at KIX because KIX is the largest among the aforementioned airports. CDO exhibit an efficient descent procedure; however, the time window during which it can be used is limited. For example, at KIX, CDO is permitted only when the estimated time of arrival (ETA) of the aircraft is between 23:00 and 7:00 in Japan local time (Japan Civil Aviation Bureau 2018) because the procedure is more unpredictable and is less controllable by air traffic controllers than the conventional method, potentially leading to disturbances in the traffic flow related to arrivals. Hence, CDO can only be performed from late night to early morning at KIX when the traffic is relatively light.

CDO procedures have also been implemented in other countries; however, these procedures also limit their applicable time to maintain a smooth traffic flow (Clarke et al. 2006). To realize the CDO procedures during daytime at Los Angeles International Airport (LAX), Clarke et al. (2013) developed an arrival procedure for which the altitude was restricted both above and below to a certain range of values, known as an altitude window. While designing an altitude window, a fast-time simulation (FTS) is iteratively conducted to evaluate the feasibility and efficiency of the designed procedure.

To enhance the operation of the CDO at the KIX, our research group investigated the feasibility of expanding the applicable time of the CDO (Hirabayashi et al. 2017). Figure 1 depicts an overview of the simulation in this study. The radar data are used to extract information about the arriving aircraft, which fly via the CDO routes; these include not only the aircraft that use CDO but also the aircraft that use conventional procedures. The authors investigated potential conflict between the extracted aircraft and the remaining aircraft in a case when a non-CDO aircraft opts to use CDO. The results depicted that more than half of the arriving aircraft that originally descended without CDO in the radar data could descend using CDO without causing any conflict. However, the vertical CDO trajectories were generated in the form of straight lines with flight-path angles of -2.2 to -2.5 degrees. By considering a variety of aircraft types, wind conditions, and other aircraft parameters, such as mass and speed during the descent phase, the CDO trajectories were observed to exhibit a high degree of variation.

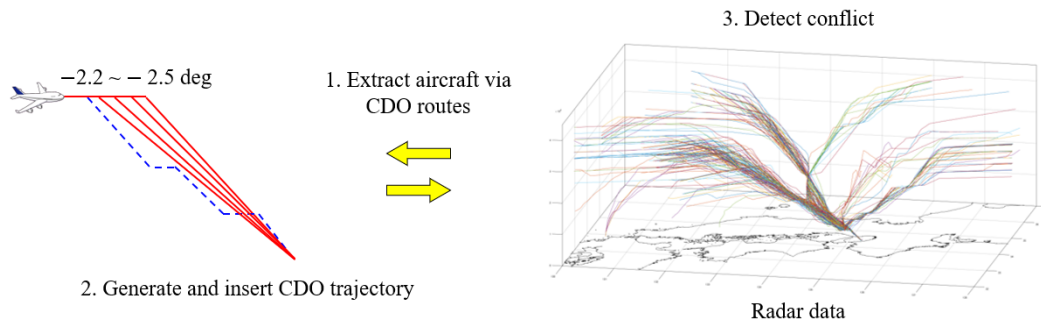


Figure 1: Overview of the simulation for investigating the feasibility of expanding the CDO operations.

The primary objective of this study is to expand the usage of CDO at KIX. One promising solution to achieve the aforementioned objective is to implement an altitude window for the CDO procedure. Our previous study investigated the feasibility of the CDO procedures using radar data; however, the vertical CDO trajectories were generated using a simple technique to investigate the feasibility. An analysis method using the trajectory that was calculated based on aircraft dynamics is required to review the altitude window; this study will exhibit the usage of such a method. The FTS is developed to review this performance based on aircraft dynamics; using the FTS, the performance metrics of efficiency and flyability can be reviewed.

The organization of this study is as follows: Section 2 explains the current CDO procedures and conditions at KIX. Section 3 describes the calculation flow of the FTS for simulating a CDO. Section 4 exhibits the calculation methodology for the investigation of the efficiency and flyability of the CDO procedure with an altitude window. Section 5 concludes and summarizes our future work.

2 CONTINUOUS DESCENT OPERATION AT KANSAI INTERNATIONAL AIRPORT

2.1 CDO Routes and Procedures

Figure 2 depicts the CDO and related approach routes for KIX. The top figure depicts the CDO routes, whereas the bottom figure depicts the standard arrival route (STAR) depicted by red solid lines and the instrument approach chart depicted by red dotted lines. KIX exhibits four CDO routes, including STAR routes, and each route has approach routes to RWY24, RWY06L, and RWY06R. For example, RWY06R CDO Number 1 starts from SUC through BECKY to ALLAN and lands at RWY06R. When an aircraft descends using the CDO procedure, it has to request for CDO for a period of ten minutes before reaching the top of descent (TOD). When this request is approved by the air traffic controllers, the aircraft can descend using the CDO. These routes are also used to perform conventional descent operations; however, in conventional operations, an air traffic controller instructs the pilots to change the altitude. For example, an aircraft flying via the same route as the CDO Number 1 without using CDO (hereinafter, this route is denoted as CDO Number 1 route) are generally instructed to cross STORK at flight level 290 (FL290) and

KARIN at FL160, owing to the fact that the air traffic controllers impose altitude restrictions to ensure smooth arrival-traffic flow. In the CDO, several altitude restrictions are cleared, and the aircraft can descend continuously.

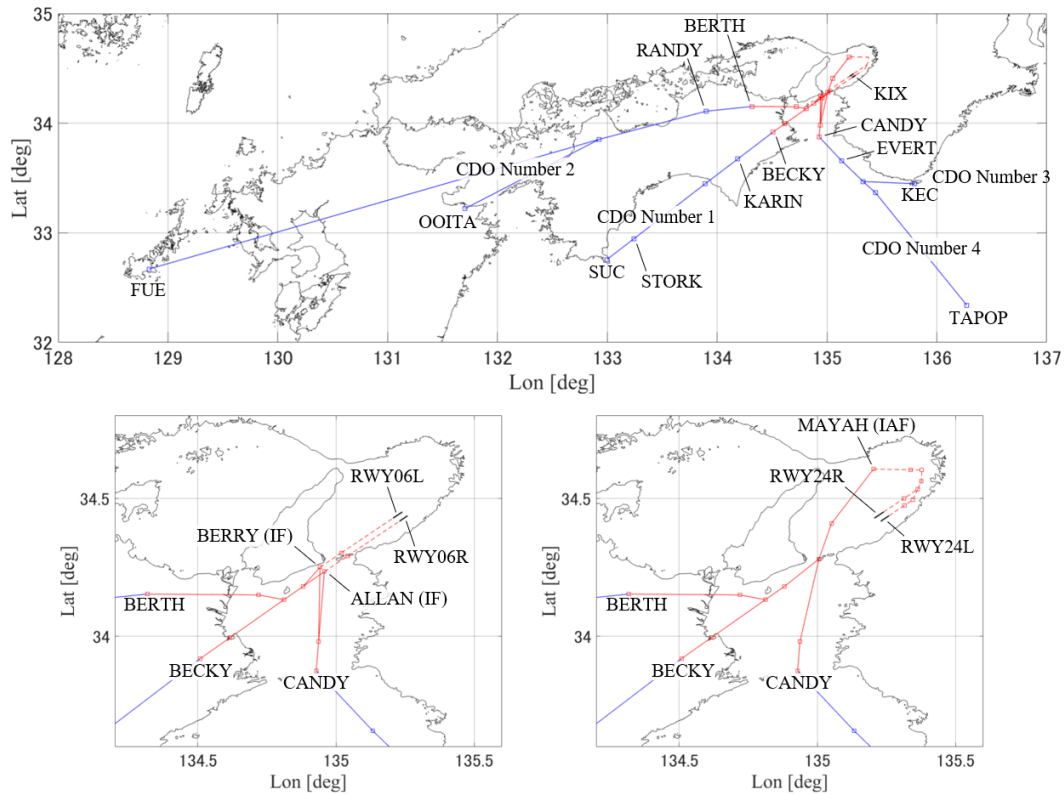


Figure 2: CDO routes for KIX.

2.2 Operational Conditions for an Arriving Aircraft at KIX

Figure 3 depicts the data for an arriving aircraft at KIX in 2017. The left pie chart exhibits the percentages of arriving aircraft at KIX using particular routes. The remaining charts depict the percentages of aircraft types that descend via the CDO routes. In these charts, the aircraft types that account for less than 5% of the data are exhibited as Other. The data are extracted from the flight data management system (FDMS) of the Japan Civil Aviation Bureau (JCAB) for a period from January 1st to December 31st, 2017. The FDMS data include flight plans that are modified with in-flight route changes. The pie charts include not only CDO aircraft but also non-CDO aircraft under current operational conditions to analyze the future operational conditions without any applicable time constraints for the CDO. The left pie chart shows that, if all aircraft arriving via the CDO routes descend using CDO, more than half of the arriving aircraft at KIX can descend using CDO. Type A aircraft are shown to be most common ones that operate on the CDO routes. The aircraft that fly through each of the CDO route are observed to originate from different directions; hence, the percentages of the aircraft types on each of the CDO route are different, as depicted by the four pie charts on the right. The vertical trajectories of different aircraft types exhibit different shapes due to differences in aircraft characteristics such as mass and speed. The difference between the percentages of aircraft types in each of the CDO route should be considered while designing the altitude window.

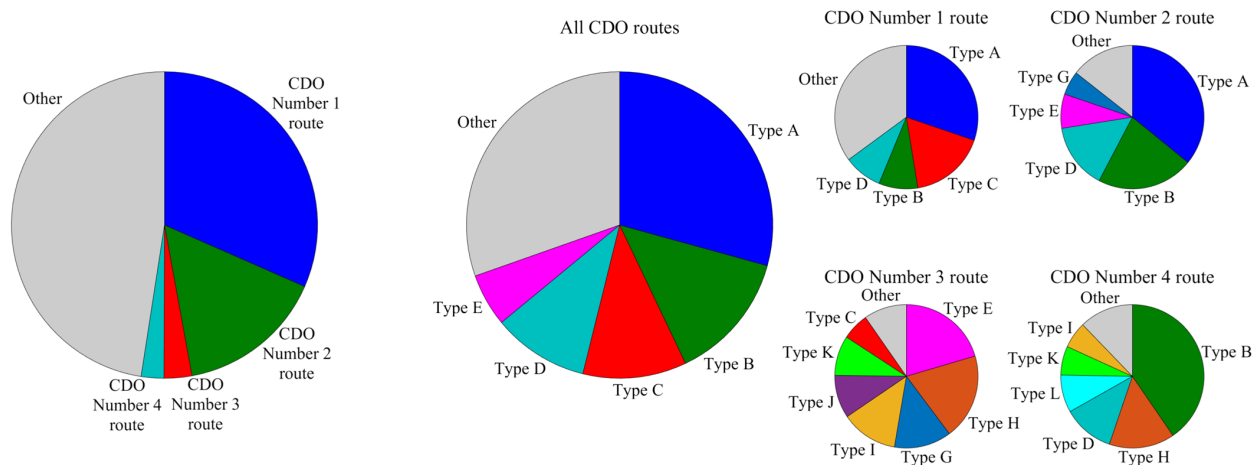


Figure 3: The percentages of aircraft using particular arrival routes and the types of aircraft arriving at KIX.

3 FAST-TIME SIMULATION

3.1 Simulation Method

An FTS is used to calculate the trajectory of a CDO aircraft (Toratani et al. 2017). Figure 4 depicts the overview of the calculation process for the FTS. In the figure, the aircraft cruises with a cruise mach number of M_{CRZ} . The aircraft begins to descend with a descent mach number of M_{DES} at the TOD. After passing the crossover altitude, the aircraft descends with CAS in the descent phase $V_{CAS,DES}$. Below an altitude of 10,000 feet, a speed limit of 250 knots is imposed on the aircraft by the Civil Aeronautics Act. To maintain this speed limit, the aircraft decelerates before reaching 10,000 feet. Below 10,000 feet, the aircraft descends, maintaining its speed below 250 knots, and connects with an approach route. The CDO aircraft maintains an idle thrust for as long as possible during its descent.

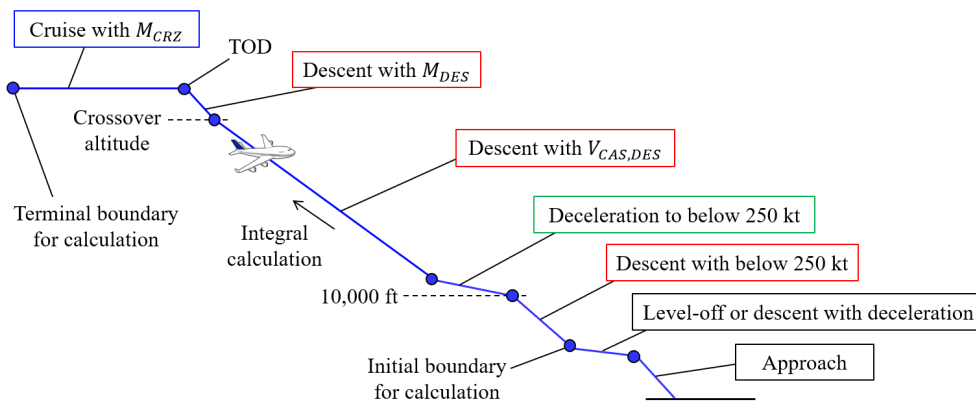


Figure 4: The FTS-calculation process for CDO trajectories.

The FTS calculates the CDO trajectory by integral calculation using the fourth-order RungeKutta method. To satisfy all the boundary conditions, the CDO trajectory is calculated in the reverse direction. In this study, the trajectory is calculated from the initial point of the CDO route to the initial approach fix (IAF) or intermediate approach fix (IF). Therefore, the IAF or IF may be set as the initial positions for the

FTS. The simulation is terminated when the trajectory reaches the initial waypoint of the CDO route. The following equation of motion is used to perform integral calculation:

$$\frac{d}{dt} \begin{pmatrix} DR \\ Hp \\ m \end{pmatrix} = \begin{pmatrix} V_{GS} \\ ROCD \\ -FF \end{pmatrix},$$

where t is time, DR is the downrange, Hp is the pressure altitude, m is the aircraft mass, V_{GS} is the ground speed (GS), $ROCD$ is the rate of climb or descent, and FF is the fuel flow. To find V_{GS} and $ROCD$, the following equation can be derived using the equilibrium of forces:

$$(Thr - D)V_{TAS} = mg_0 \frac{T}{T - \Delta T} ROCD + mV_{TAS} \frac{dV_{TAS}}{dt},$$

where Thr is the engine thrust, D is the aerodynamic drag, V_{TAS} is the true air speed (TAS), g_0 is the gravitational acceleration, T is the atmospheric temperature, and ΔT is the temperature difference from International Standard Atmosphere (ISA). Generally, the aircraft is controlled by specifying two of the three variables that are as follows: Thr , speed, and $ROCD$ (Bronsvort 2014). The speed is specified as M or V_{CAS} and is transformed to V_{TAS} . For example, while cruising, the speed that is specified as M_{CRZ} , $ROCD$ is set to 0, and Thr can be calculated using the equation of equilibrium. In this case, the speed and $ROCD$ are called the controlled states, whereas Thr is called an open state. While the aircraft descends with a constant speed, as depicted by the red box in Fig. 4, the speed and Thr are the controlled states, whereas $ROCD$ is an open state. When the aircraft decelerates, as depicted using the green box, Thr and $ROCD$ are the controlled states, whereas the speed is an open state. The base of aircraft data 4 (BADA4) is used to derive FF , D , and the idle thrust Thr_{idl} . BADA4 has been developed by EUROCONTROL and provided several equations and coefficients for calculating the performance of each aircraft and the engine type (EUROCONTROL Experimental Center 2014). The FTS can consider the differences between aircraft types using BADA4; additionally, numerical weather prediction (NWP) data are used to simulate the wind conditions. NWP is provided by the Japan Meteorological Agency (JMA) and comprised the observed and forecast data that was estimated using the following two models: a global spectral model (GSM) and a mesoscale model (MSM). V_{TAS} is transformed into V_{GS} using the wind velocity for the integral calculation.

3.2 Simulation Examples

As an example, a CDO trajectory is depicted in this section; the route is set as the RWY06R CDO Number 1, and the aircraft type is set as Type A. Figure 5 depicts the sample wind data around the CDO routes at

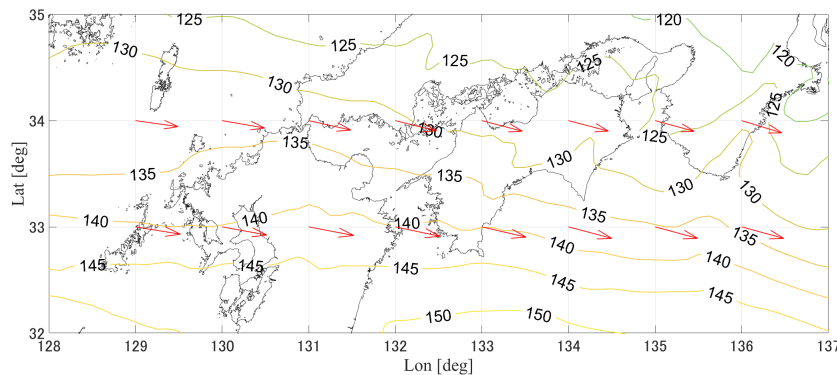


Figure 5: Sample wind data.

KIX. The MSM data are used during this simulation. The figure depicts the wind at 200 hPa and at 00:00 on January 1st, 2017. The contour lines exhibit the wind velocity in knots, whereas the red arrows exhibit the wind direction. The sample data depict that the Japanese airspace generally has a high west wind. Figure 6 depicts the wind distribution at each altitude. The left and right figures illustrate the zonal wind, V_{wx} , and the meridional wind, V_{wy} , respectively. The observed MSM data are collected from all the days and times in 2017. The distribution also depicts that there is a strong west wind. The meridional wind is less distributed than the zonal wind, and its median is approximately zero, regardless of the altitude. The FTS calculates the wind as a layer at every 5,000 feet, except at the bottom layer. The atmospheric conditions are set as ISA.

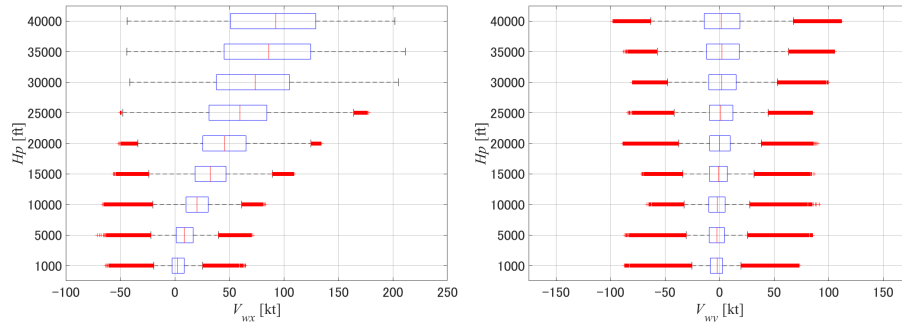


Figure 6: Wind distribution in the simulation area.

Figure 7 depicts the results of the simulation example. In this simulation, the results of the CDO are compared with those of the conventional descent procedure to exhibit the potential benefit of the CDO. The solid line depicts the CDO, whereas the chained line depicts the conventional descent. Each figure illustrates the horizontal trajectory, vertical trajectory, speed, rate of climb or descent, thrust, and fuel flow. The boundary conditions, including the terminal aircraft mass, m_f , and $V_{CAS,DES}$, are set as the representative values. The wind conditions are set as the median values that are depicted by the red bars in Fig. 6. The conventional descent imposes altitude restrictions at STORK and KARIN maintaining at FL290 and FL160, respectively. The total fuel consumptions of the conventional and continuous descent operations are 1,177 and 1,041 pounds, respectively. Thus, the CDO can reduce the fuel consumption by 136 pounds in this case. The succeeding section depicts the methodology for utilizing the FTS to investigate the CDO operations.

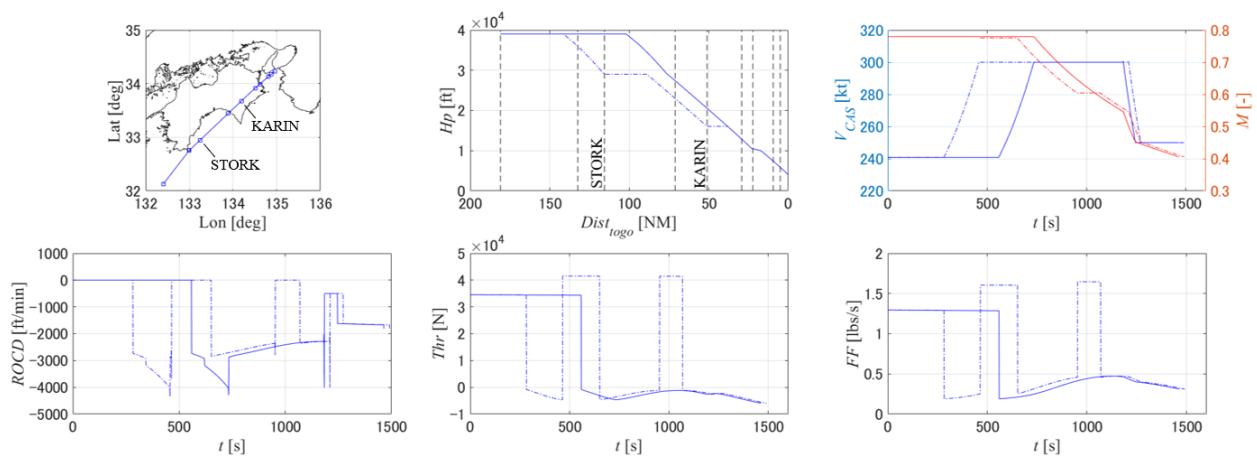


Figure 7: Results of the simulation example.

4 SIMULATION METHODOLOGY FOR INVESTIGATING THE CDO

4.1 Variation of the Vertical Trajectory

According to Xue and Erzberger (2011), the vertical trajectory of the CDO aircraft mainly depended upon its type, mass, speed in descent phase, and wind speed. One problem that is encountered while expanding the applicable time for the CDO is the unpredictability of the CDO trajectory. Hence, it is important to derive the maximum range of this trajectory. Figure 8 depicts the variation of the CDO trajectories based on the parameters that were mentioned above. The left figure depicts the variation of the CDO trajectories between different aircraft types. The same simulation conditions that are exhibited in Section 3.2 are applied to all the aircraft types. Herein, the simulation condition is denoted as a nominal condition, whereas the resultant trajectory is denoted as the nominal trajectory. The figure includes the trajectories of the top four aircraft types in CDO Number 1 route, as depicted in Fig. 3. BADA4 provides the models of each aircraft type with several types of engine. The aircraft types with different engine models are denoted as Types A-1 to A-4. The results exhibit that different vertical trajectories are yielded for different aircraft types. For example, Types B-1 to B-3 have shallower trajectories than the others. The same aircraft types with different engines have basically similar trajectories; however, Type A-1 deviates from other Type A aircraft. In the right figure, Type A-2 is set as the aircraft type, and the simulation conditions are set in accordance with Section 3.2, except for the m_f , $V_{CAS,DES}$, and the wind conditions. Light aircraft mass, high CAS in the descent phase, and head winds yield steeper descent trajectories, whereas heavy mass, low CAS, and tail winds yield shallower trajectories. The bold dotted lines are the maximum range of the CDO trajectory with Type A-2. The nominal trajectory of Type A-2 is also considered as a reference. To derive the upper trajectory (which is the steepest descent), m_f and $V_{CAS,DES}$ are set as $1.2 \times$ the operational empty weight (OEW) and the maximum operating speed (V_{MO}) that is provided by BADA4. The wind conditions are set as the values on the left whiskers that are depicted in Fig. 6 to set the head wind. The lower trajectory is derived using the maximum landing weight (MLW) as m_f , with a $V_{CAS,DES}$ of 250 knots and wind conditions that are given by the values on the right whiskers. The results depict that the variation of the CDO trajectories due to aircraft mass, CAS in the descent phase, and wind speed is larger than that caused due to the aircraft type. By combining both the simulations and by considering the aircraft type, mass, CAS, and wind, the maximum range of the vertical CDO trajectory in CDO Number 1 route can be derived. However, each parameter for deriving the maximum range is an extreme value. An aircraft can descend with V_{MO} ; however, almost no aircraft can fly at such a high speed. Regarding the wind conditions, the probability distribution around KIX can be derived as depicted in Fig. 6. If the probability distribution of mass and speed in the CDO conditions at KIX can be obtained, it can be used to find the probability distribution of vertical trajectories.

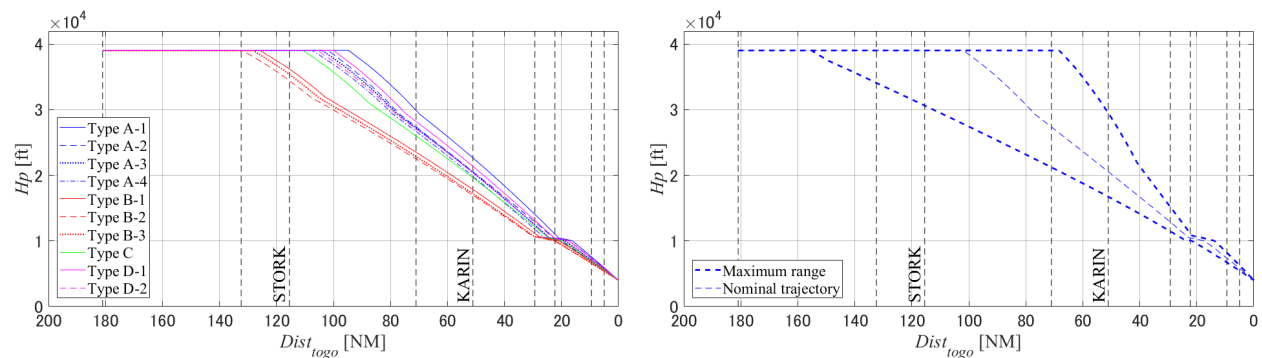


Figure 8: Variation of the CDO trajectories (left: variation from aircraft types; right: the maximum range of CDO trajectories for Type A-2).

4.2 Review Methodology for the Altitude Window

As depicted in Fig. 8, the possible vertical trajectory of the CDO exhibits a wide range. This range makes the CDO aircraft to be unpredictable for air traffic controllers. The altitude window is a constraint upon the vertical trajectory; accordingly, this window can increase the predictability of arrival traffic flow. However, the flyability of an aircraft arriving at KIX must be investigated to introduce this altitude window; unless this is done, the altitude window may impose unreasonable flights on the arriving aircraft. For example, with too steep altitude window, some aircraft would not be able to descend reasonably. An aircraft that descends with an idle thrust can steepen its flight-path angle with acceleration. If the altitude window is too steep for the aircraft, even with V_{MO} , it will have to use a speed brake to maintain an altitude window. The usage of speed brake is an undesirable operation for the pilot. Further, the efficiency of the altitude window should be investigated to ensure that the fuel is not wasted. If the altitude window is too shallow, the aircraft requires additional thrust besides the idle thrust to maintain a shallower flight-path angle with consuming additional fuel. This section depicts the methodology used to review the flyability and efficiency of the designed altitude window.

As an example, two configurations of the altitude window are set, as presented in Table 1. Both the configurations have the same range that are as follows: 6,000 feet at STORK and 2,000 feet at KARIN; however, Config 1 is steeper than Config 2. To simplify this problem, the trajectory below 10,000 feet is fixed with an additional altitude restriction of 10,000 feet at BECKY. The FTS is modified to review the altitude window. If the CDO trajectory falls within the altitude window, the calculation process that is depicted in Fig. 4 is used. If the original CDO trajectory spills out from the altitude window, the aircraft keeps its ground-related flight-path angle γ_{GS} constant to descend along the altitude window while maintaining the speed as M_{DES} or $V_{CAS,DES}$, as depicted in Fig. 9. Further, the required thrust can be derived from the equation of equilibrium between forces, as mentioned in Section 3.1.

Table 1: Configurations of the altitude window.

Waypoint	STORK	KARIN	Waypoint	STORK	KARIN
Config 1	Below FL380	Below FL170	Config 2	Below FL310	Below FL160
	Above FL340	Above FL150		Above FL270	Above FL140

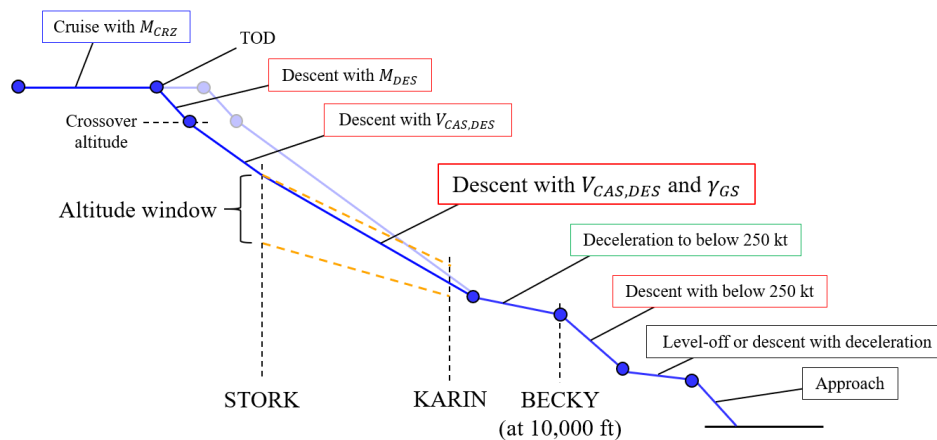


Figure 9: Calculation process for CDO trajectory with an altitude window.

Figure 10 depicts the simulation results with the altitude windows. The left figure presents the vertical trajectories with Config 1, whereas the right figure presents that with Config 2. The altitude windows are depicted by the orange lines at STORK and KARIN. The simulation conditions are set as nominal conditions. By comparing the left figure of Fig. 8, both the altitude windows can suppress the range of

the vertical trajectories. With Config 1, only Type C can descend with the original CDO trajectory. Types B-1 to B-3 hit the lower boundary of the altitude window, whereas the other types hit the upper boundary. With Config 2, all the aircraft hit the upper boundary at STORK. Before STORK, their flight-path angles are steeper than they are between STORK and KARIN; this indicates that Config 2 is shallower than all the nominal trajectories. To depict the efficiency of the altitude windows, Table 2 presents the additional fuel consumption that is caused due to this window. The flight with the altitude window consumes more fuel than that consumed by the original CDO flight because every aircraft deviates from the original CDO trajectory except for Type C in Config 1. There are no available data regarding the percentages of aircraft engine types in CDO Number 1 route; therefore, additional fuel consumption for each aircraft type is averaged for all the engine types. To compare the two configurations of the altitude windows, the average additional fuel consumption is weighted based on the percentages of aircraft types in CDO Number 1 route, as depicted in Fig. 3. The additional fuel consumption of Config 1 is lower than that of Config 2. The results depict that Config 1 has high fuel efficiency; however, the flyability must also be considered.

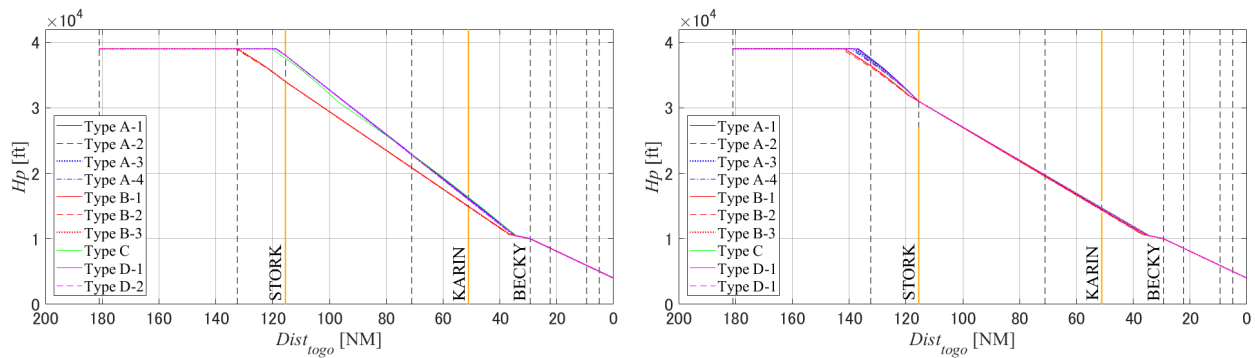


Figure 10: Vertical trajectories with an altitude window (left: Config 1; right Config 2).

Table 2: Additional fuel consumption due to altitude window.

Aircraft type	A	B	C	D	Weighted average
Percentages in CDO Number 1 route[%]	30.2	17.2	8.8	8.7	-
Additional fuel consumption (Config 1) [lbs]	10.9	11.2	90.7	0.0	32.6
Additional fuel consumption (Config 2) [lbs]	80.9	74.0	65.8	37.8	74.7

Figure 11 illustrates the thrust for the Type B-1 aircraft in the case that is depicted in Fig. 10. The solid line is the time history of the thrust, whereas the chained line is the idle thrust provided by BADA4. In Config 1, the thrust required to stay within the altitude window would be lower than the idle thrust between

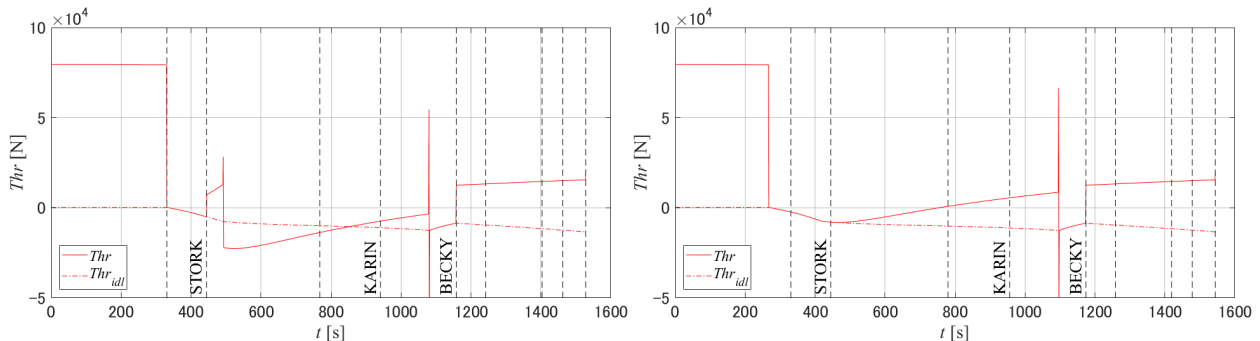


Figure 11: Thrust for Type B-1 (left: Config 1; right Config 2).

STORK and KARIN. It indicates that the aircraft needs to use the speed brake to compensate for the excess thrust. However, the thrust in Config 2 does not exceed the idle thrust. Concerning the other aircraft types, several of them have to use speed braking in Config 1; however, none of the aircraft use speed brakes in Config 2. In this study, the case in which the altitude window imposes the usage of the speed brake is said to have low flyability; hence, the flyability of Config 1 is lower than that of Config 2. The results depict that there is a trade-off between efficiency and flyability in the design of the altitude window. In this section, only the nominal conditions are reviewed as an example; however, further investigation with other conditions, including differing mass, speed, and wind, are required for designing the altitude window.

4.3 Discussion

In the previous sections, the review methodology for designing the altitude window is depicted along with the maximum possible range of the CDO vertical trajectory. However, as mentioned in Section 4.1, almost no aircraft descend at the steepest or shallowest trajectories; the edges of the maximum range are depicted in Fig. 8. The vertical trajectory of the CDO aircraft depends upon the aircraft type, mass, speed, and wind speed. The percentages of aircraft types in CDO Number 1 route and the probability distribution of the wind, as depicted in Fig. 6, are available among them. Using the probability distributions of the aircraft's mass and speed, the vertical trajectory can be expressed as a probability distribution. To design the altitude window, the review methodology for the altitude window has to investigate all the possible trajectories if only the maximum range of the CDO trajectory is available; however, using the probability distribution of the vertical trajectory, the review range can be reduced. Additionally, the altitude window can be designed based on more convincing bases by considering the probability distribution.

The target of the review methodology for the altitude window is to investigate the fuel consumption (efficiency) and the reasonability of aircraft dynamics (flyability). The efficiency and flyability represent the performance of the altitude window with regard to each flight. Hence, they are collectively referred to as the aircraft-oriented performance in this study. The research illustrated in Fig. 1 investigates the feasibility of air traffic control (ATC); namely, the ATC-oriented performance. An altitude window suitable for the real operational conditions of the CDO can be designed by repeating the aircraft- and ATC-oriented reviews, as depicted in Fig. 12. However, the ATC-oriented review method shown in Fig. 1 investigates only whether an aircraft experiences conflict without ATC instructions in a case where all the aircraft descend using the

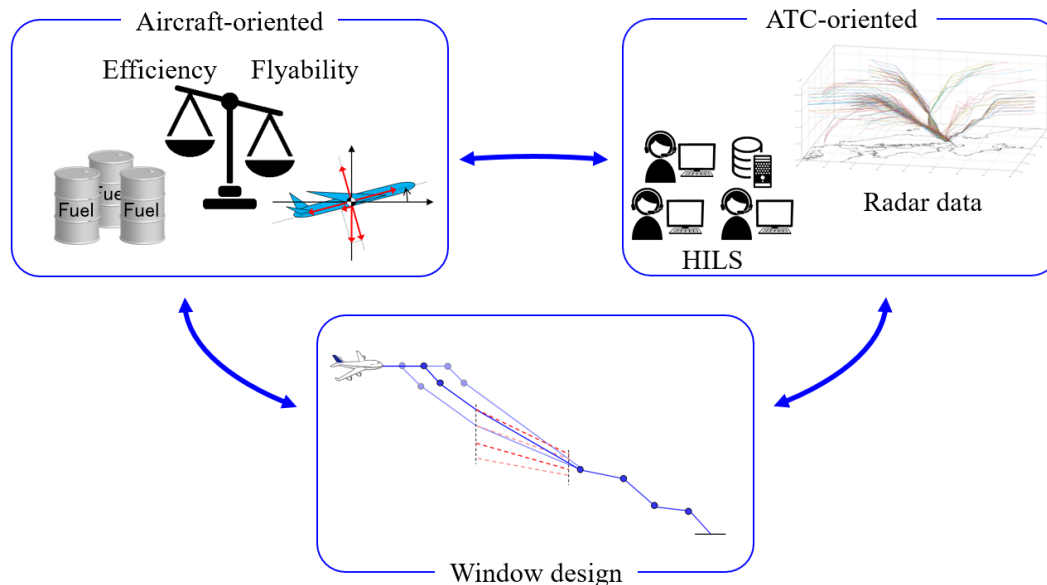


Figure 12: Schematic of the design process for the altitude window.

CDO. If this potential conflict can be resolved by the ATC instructions, the CDO is still feasible from the point of view of the ATC. To complete the design process, the ATC-oriented review should also include investigation of whether the CDO can arrive without conflict using ATC instructions, for example, using a human-in-the-loop simulation (HILS). Further, the design process can appropriately review the ATC-oriented performance of the altitude window.

5 CONCLUSION

This study presented the simulation techniques for the design of the CDO procedure. The FTS was used to investigate the maximum possible range of the vertical CDO trajectory and to review the performance of the altitude window. The review methodology for the altitude window investigated the efficiency and flyability. In exemplary simulations, steeper altitude windows were observed to exhibit better efficiency than that exhibited by shallower ones (i.e., they consumed less fuel). However, the shallower altitude window depicted better flyability than that depicted by the steeper window; this window does not require the usage of the speed brake for the aircraft. The design process for the altitude window, including the review methodology, was discussed.

Our future study will aim to improve the ATC-oriented-review methodology. As mentioned in Section 4.3, the design process should review whether the aircraft can descend using the CDO without conflict. In particular, the ATC-oriented review must investigate whether the CDO aircraft can resolve the conflict using the ATC instructions. By improving the review methodology, the design process can develop the altitude window by considering the feasibility for each flight and ATC.

ACKNOWLEDGMENTS

Authors would like to acknowledge the Japan Civil Aviation Bureau for providing radar and FDMS data, and the BADA Team of Eurocontrol for providing valuable technical advice.

LICENSE AGREEMENT

This product or document has been created by or contains parts which have been created or made available by the European Organization for the Safety of Air Navigation (EUROCONTROL). EUROCONTROL ©2013. All rights reserved. EUROCONTROL shall not be liable for any direct, indirect incidental or consequential damages arising out of or in connection with this product or document, including with respect to the use of BADA4.

REFERENCES

- Bronsvoort, J. 2014. *Contributions to Trajectory Prediction Theory and its Application to Arrival Management for Air Traffic Control*. Ph. D. thesis, Technical University of Madrid.
- Clarke, J.-P. B., D. Bennett, K. Elmer, J. Firth, R. Hilb, N. Ho, S. Johnson, S. Lau, L. Ren, D. Senechal, N. Sizov, R. Slattery, K.-O. Tong, J. Walton, A. Willgruber, and D. Williams. 2006. "Development, Design, and Flight Test Evaluation of a Continuous Descent Approach Procedure for Nighttime Operation at Louisville International Airport". In *Report of the PARTNER Continuous Descent Approach Development Team*, Number Report No. PARTNER-COE-2006-002.
- Clarke, J.-P. B., J. Brooks, A. S. G. Nagle, W. White, and S. R. Liu. 2013. "Optimized Profile Descent Arrivals at Los Angeles International Airport". *Journal of Aircraft* 50 (2): 360–369.
- EUROCONTROL Experimental Center 2014. *User Manual for the Base of Aircraft Data (BADA) Family 4*. EUROCONTROL Experimental Center. EEC Technical/Scientific Report No. 12/11/22-58.
- Hirabayashi, H., S. Fukushima, M. Oka, N. K. Wickramasinghe, and D. Toratani. 2017. "Feasibility Study on the Expansion of Continuous Descent Operations (CDO) at Kansai International Airport with Track Data Analysis". In *Proceedings of the 55th Aircraft Symposium*.

- International Civil Aviation Organization 2010. *Continuous Descent Operations (CDO) Manual*. International Civil Aviation Organization. Doc 9931.
- Japan Civil Aviation Bureau 2018. “eAIP Japan, RJBB AD 2.20, LOCAL TRAFFIC REGULATIONS”. <https://aisjapan.mlit.go.jp/html/AIP/html/20180329/eAIP/20180401/JP-AD-2-RJBB-en-JP.html#AD-2.RJBB>. Accessed data: 9 April 2018.
- Toratani, D., N. K. Wickramasinghe, S. Fukushima, and H. Hirabayashi. 2017. “Design Methodology to Simulate Continuous Descent Operations at Kansai International Airport”. In *In the proceedings of 2017 Winter Simulation Conference (WSC)*, 2578–2588, edited by W.K.V. Chan et al., Piscataway, New Jersey : IEEE.
- Xue, M., and H. Erzberger. 2011. “Improvement of Trajectory Synthesizer for Efficient Descent Advisor”. In *Proceedings of the 11th AIAA Aviation Technology, Integration, and Operations (ATIO) Conference*.

AUTHOR BIOGRAPHIES

DAICHI TORATANI is a researcher at the Air Traffic Management Department of the Electronic Navigation Research Institute (ENRI) in Japan. He holds a Ph.D. in Engineering from Yokohama National University, Kanagawa, Japan. His research interests include optimization, control, simulation and its applications in air traffic management, and unmanned-aircraft systems. His e-mail address is toratani-d@mpat.go.jp.

NAVINDA KITHMAL WICKRAMASINGHE is a researcher at the Air Traffic Management Department of the Electronic Navigation Research Institute (ENRI) in Japan. He holds a Ph.D. in Engineering from Kyushu University, Fukuoka, Japan. His research interests include aircraft-performance modeling, aircraft-noise abatement, and optimal control applications in 4D-trajectory-based operations. His e-mail address is navinda@mpat.go.jp.

HIROKO HIRABAYASHI is a senior researcher at the Air Traffic Management Department of the Electronic Navigation Research Institute (ENRI) in Japan. She received her Master’s degree in Science from Yokohama City University, Kanagawa, Japan, in 1997. She worked as an air traffic controller for 15 years. Her research interests include big data analysis and fast-time simulations on technical approaches for safe and efficient air-traffic operations. Her e-mail address is h-hirabayashi@mpat.go.jp.